RESPONSE OF ASCE TASK COMMITTEE TEST CASES TO OPEN-LOOP CONTROL MEASURES

By E. Bautista,[1] Associate Member, ASCE and A. J. Clemmens,[2] Member, ASCE

ABSTRACT: Automated open- and closed-loop control systems can enhance the performance of irrigation delivery systems. This paper examines the response of the canal test cases developed by the ASCE task committee on canal automation algorithms to a particular anticipatory open-loop control technique, gate stroking. The performance of the ideal gate-stroking solution is compared with the performance of an approximate gate-stroking schedule that was generated by imposing practical constraints on the frequency and magnitude of the gate adjustments. Also analyzed were the performance of a nonanticipatory open-loop control scheme and the effect of model parameter uncertainties on the effectiveness of the control. For the test cases, the approximate gate-stroking schedules performed similarly to the ideal schedules. For two of the test cases, delivery performance was similar with and without anticipation, but was substantially different for the other two tests. The quality of the control degraded as a result of errors in model parameters, particularly in cases with incorrect check gate calibrations and submerged gate flows. Results point out the importance of combining open- and closed-loop control measures to improve the overall effectiveness of the control.

INTRODUCTION

Feedback (closed-loop) control methods offer one alternative for enhancing the flexibility and reliability of water deliveries to agricultural users. In turn, improved water deliveries can facilitate water resource management at the farm level. Feedback control alone, however, may be unable to provide adequate flow control because upstream flow changes travel downstream at a finite speed. The magnitude of the resulting delay in response depends on the canal's physical characteristics and the initial flow conditions. Because for many delivery systems demand changes can be predetermined, canal control systems that include both feedforward (anticipatory, open-loop control of flow rates) and feedback (closed-loop control of downstream water level) control measures can provide a more flexible and reliable water delivery service.

An ASCE task committee on canal control algorithms was formed in 1993 to promote the development and implementation of canal control methodologies (Clemmens et al. 1998). This committee developed canal control test cases that could be used to compare the performance of proposed algorithms under standard conditions. This paper examines the response of these test cases to gate stroking (Wylie 1969), a feedforward control technique. Gate stroking is a computational procedure for determining a schedule of canal inflows that will deliver a prespecified demand. The method is based on the solution of the Saint-Venant equations of unsteady open-channel flow and can also be described as an inverse computational method. The basic gate-stroking method assumes that control structures can be manipulated continuously in time to deliver the exact flows required by the numerical solution. Further, it also assumes that accurate estimates of the canal's hydraulic parameters are available. Often, these two assumptions are difficult to satisfy under field conditions. Thus, there are two additional objectives to this paper. The first is to examine how the performance of the gate-stroking control degrades when the computed schedules are implemented in approximate form. The second

is to test the effect of inaccurate model parameters on the quality of the gate-stroking solution.

METHODOLOGY

Inverse Computations

Inverse solutions of the unsteady flow equations begin at the downstream boundary of the canal where depth and discharge variations with time are specified. Computations proceed backward in space, solving for the corresponding depth and discharge hydrographs at the upstream boundary of the system. The corresponding gate-opening changes are determined from the control structure's head-discharge relationship. As in routing application of the Saint-Venant equations, gate-stroking solutions need to be obtained numerically. Solution procedures have been developed based on the method of characteristics (Wylie 1969; Falvey and Luning 1979) and on finite differences (O'Laughlin 1972; Chevereau 1991; Liu et al. 1992; Bautista et al. 1997).

A nonlinear implicit finite-difference gate-stroking algorithm (Bautista et al. 1997) was adopted for this study. This algorithm combines good numerical accuracy and robustness properties relative to alternative approaches. The procedure is based on the Preissman four-point finite-difference scheme and solves simultaneously for a group of points along a space line. The method requires steady-state flow conditions prior to the initiation of the transient.

Because the inverse solution generates a sequence of depths and discharge hydrographs as it progresses from one spatial node to the next, linking computations between adjacent pools is a straightforward process. In a canal system with N pools, from continuity, the inflow hydrograph computed at the upstream end of pool N provides the corresponding outflow (downstream) hydrograph for pool $N - 1$. The user specifies the constant target depths to be maintained during the transient at the downstream end of each pool. This process is repeated until reaching the most upstream pool. Because the depths upstream from gates are specified, calculations at the boundary between two pools can be carried out independently from the gate head-discharge calculations. The gate head-discharge relationship can be used subsequently to determine the gate openings from the computed flow rates.

Task Committee Test Cases

A complete description of the task committee canal regulation test cases is available in Clemmens et al. (1998). The

[1] Agric. Engr., U.S. Dept. of Agric.-ARS, U.S. Water Conservation Lab., 4331 East Broadway Rd., Phoenix, AZ 85040.

[2] Dir., U.S. Dept. of Agric.-ARS, U.S. Water Conservation Lab., 4331 East Broadway Rd., Phoenix, AZ.

examples consist of two canals, labeled Canal 1 and Canal 2, the first of which is steep and has a low storage volume, while the second has a milder slope and greater storage volume. The first canal is 9.5 km long, and the second 28 km. Each canal consists of eight pools separated by underflow gates. Each pool, in turn, has a turnout near the downstream boundary. The objective of the control tests is to maintain the target depth at each pool forebay while delivering the specified changes in turnout flow. Values for the target depths are given in Tables 2 and 3 of Clemmens et al. (1998), while Tables 4–7 in the same reference list the turnout flow rate variations. The complete set of tests considers both scheduled and unscheduled flow changes. Because the gate-stroking solution can only handle scheduled water deliveries, the response to unanticipated changes is not relevant to this study. Therefore, the present study only examines conditions specified for the first 12 h of the task committee test cases.

Two control scenarios were examined for each canal, both starting from steady state. The first scenario consists of a step change in discharge at two turnouts, with both changes occurring at time $t = 2$ h. In the second scenario, six of the eight turnouts undergo changes in flow, also at $t = 2$ h. In the following discussion, the labels 1-1, 1-2, 2-1, and 2-2 identify each control test, with the first number referring to the canal number the second to the scenario.

The gate-stroking solutions require continuous operation of the canal gates and gate-opening resolutions that are as precise as the computer results. In reality, continuous operation of gates, which requires variable-speed gate motors, is impractical and gate displacement cannot be controlled with the precision assumed by the computer calculations. Previously, Bodley and Wylie (1978) examined the performance of approximate gate-stroking schedules developed using single- or two-speed gate motors. In their tests, the approximate solution performed satisfactorily in comparison with the ideal solution. This study compares the performance of the ideal gate-stroking solutions with the performance of an approximate solution derived based on operational constraints imposed by the task committee test cases. In the test cases, gate changes are allowed only at discrete time intervals and only if the requested gate-opening change is greater than or equal to a minimum value. The task committee recommended regulation time interval is 5 and 15 min, for Canals 1 and 2, respectively, whereas the limit for minimum gate changes is about 0.5% of the gate height. Constant minimum gate changes of 0.005 m for all gates in Canal 1 and of 0.01 m for all gates in Canal 2 were adopted for this study.

As stated previously, hydraulic property information, such as roughness and the gate head-discharge relationship, may not be accurately known at the controller design time and can be expected to change with time. Given this uncertainty, it is important to examine the sensitivity of a control algorithm to hydraulic parameter calibration errors. To this end, the task committee recommended testing the control algorithms with tuned and untuned parameters. In this paper, the untuned tests were carried out by routing the gate-stroking solutions with values of Manning's n and gate discharge relations different from those used in the inverse calculations. Manning's n values used in the gate-stroking calculations were 0.14 for Canal 1 and 0.2 for Canal 2. These values were increased to 0.18 and 0.26 for the routing calculations. The gate head-discharge relationship was modified by reducing the horizontal contraction coefficient [(1 and 2)] from 1.0 (for the gate-stroking calculations) to 0.9 (for the routing or forward simulation).

Development of Gate-Stroking Solutions

The model of Bautista et al. (1997) was used to calculate depth and flow hydrographs at each gate. Calculations were carried out with a 1 min time step for both canals. The computational space step for Canal 1 was between 200 and 212.5 m for all pools except the first, where a 50-m step was used. For Canal 2, a 500-m space step was used for all pools. In the following discussion, these solutions are identified as the ideal schedules. Approximate schedules were developed based on the volume of water delivered by the ideal schedules over each regulation period. The approximate schedules were computed as follows: The ideal pool outflow hydrograph was integrated to obtain a total discharge volume. This total volume was divided by the time interval to obtain the average flow rate for the regulation interval. Next, average depth was computed at the upstream boundary of the next pool (i.e., the afterbay depth) for the same time interval. A gate opening for the regulation interval was computed from the average discharge, average afterbay depth, and the target forebay depth. A gate movement was scheduled whenever the absolute difference between the computed opening and the current gate opening exceeded the gate change constraint. If the difference did not exceed the constraint, then a volume to be delivered during the current regulation interval and with the current (unchanged) gate settings was computed. The difference between this volume and the volume computed from integrating the gate-stroking solution was stored and added to the volume computed for the following regulation period. This cumulative volume was then used to compute the average flow rate for the following regulation time interval.

Because of the constraint on the minimum gate movement, and because changes in flow rate become very small near the end of the transient, the computed gate positions tend to oscillate around the desired final steady-state gate opening. To prevent this oscillation, the computed gate openings were adjusted to match the final desired opening whenever the difference between computed and target values was less than the minimum gate movement. While this approach results in a final gate movement smaller than the minimum specified by the task committee, its use can be justified by the fact that the control algorithm being examined is of an open-loop type, whereas the test cases were designed with closed-loop algorithms in mind. Without this final adjustment, water levels will necessarily drift because pool inflows will not match exactly the requested outflows.

Verification of Gate-Stroking Solutions

The inverse model results were verified through simulation with CanalCAD (Holly and Parrish 1995), an unsteady flow model. CanalCAD, like the previously described inverse model, uses the Preissman four-point scheme to discretize the Saint-Venant partial differential equation system. The program determines internally an appropriate time/space step combination to use in the calculations, although the user can specify a maximum time interval. For this study, all simulations were conducted with a 1-min maximum time interval. The test cases do not specify either the check gate or turnout flow head-discharge relationships. Therefore, CanalCAD's default equations were adopted for this study. These equations are described next.

Gate and Turnout Equations

CanalCAD's default underflow gate-discharge relationships (Holly and Parrish 1995) are

$$Q_G = \mu \varepsilon B a \sqrt{2g} \sqrt{y_{us} - y_s - \frac{a}{2}} + Q_l \qquad (1)$$

$$Q_G = \mu \varepsilon B a \sqrt{2g} \sqrt{y_{us} - y_{ds}} + Q_l \qquad (2)$$

the first of which applies under free-flowing conditions and the second under submerged conditions. In this formulation, free-flow conditions exist if the downstream water level is less than the elevation of the gate opening midpoint. Variables in (1) and (2) are defined as follows: Q_G = gate discharge; a = gate vertical opening; B = gate width; ε = dimensionless variable vertical contraction coefficient; μ = dimensionless constant horizontal contraction coefficient; y_{us} = depth upstream from the gate; y_{ds} = depth downstream of the gate; y_s = gate sill elevation relative to the canal invert; and Q_l = gate leakage (assumed constant). For the test cases, y_s and Q_l are both equal to zero. Values for the variable vertical contraction coefficient are computed as follows:

$$\varepsilon = 0.65 \quad \text{for } 0.0 \leq a/H \leq 0.55 \qquad (3)$$

$$\varepsilon = 0.5 + 0.268\,\frac{a}{H} \quad \text{for } 0.55 \leq a/H \leq 0.9 \qquad (4)$$

$$\varepsilon = 0.745 + 2.55\left(\frac{a}{H} - 0.9\right) \quad \text{for } a/H > 0.9 \qquad (5)$$

where H = upstream depth above the gate sill

$$H = y_{us} - y_s \qquad (6)$$

which for the test cases is equal to y_{us}.

CanalCAD uses an orifice-type relationship to compute the turnout discharge q

$$q = K(y - y_0)^x \qquad (7)$$

where K = product of the discharge coefficient, the orifice area, and $(2g)^{1/2}$; y = depth in the canal upstream from the turnout; y_0 = depth downstream from the turnout, which was taken as half of the target depth for the test cases; and x = constant discharge exponent, which is typically given a value of 0.5. K is computed internally by the program for the user-specified target Q_{TO}, target y, and y_0. Because the test cases specify a short distance (5 m) between the turnout and gate, the target depth upstream from the turnout was made equal to the target downstream pool depth.

RESULTS AND DISCUSSION

Delivery Performance of Ideal Gate-Stroking Schedules

Fig. 1 depicts the ideal canal inflow (thick solid line) and gate-opening schedules (thin lines) derived for each test case. Because inflow and gate positions reached their final steady-state values before $t = 3$ h for all test cases, the graphs show only the initial portion of the schedule. In Fig. 1, the time axis for Test 2-2 was extended to the left of $t = 0$ h to show the initial inflow change that occurs more than 2 h in advance of the scheduled change.

As expected, the ideal gate-stroking solutions (Fig. 1) show that adjustments are required only at control structures upstream from the most downstream turnout with a prescribed flow change. Control structures downstream from this last turnout with a change do not need to be adjusted. Ideally, depth and discharge at pools downstream from the last affected pool should also remain unchanged.

Fig. 2 and 3 show the difference between the CanalCAD simulated depths and offtake flows, based on the ideal gate-stroking solutions, and their corresponding targets. If both the gate-stroking and routing results were exact, simulated downstream water levels would remain constant throughout the transient while discharge through the check structures would vary as needed to meet the changes in offtake demand. However, both sets of results are subject to numerical inaccuracies, and therefore, the simulated levels and offtake flows deviate
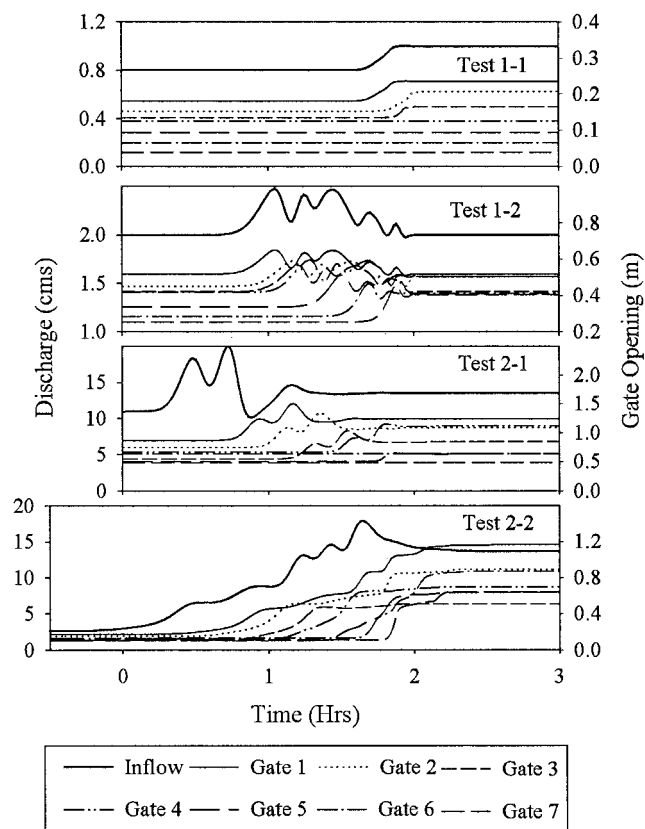

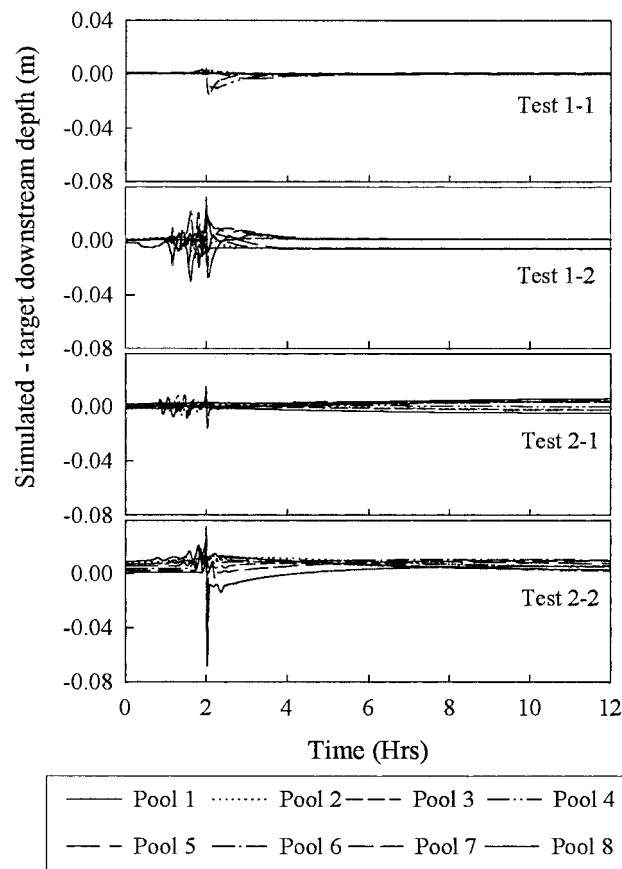**FIG. 1. Ideal Inflow and Gate-Opening Schedules Computed with Gate-Stroking Model**

FIG. 2. Difference between Simulated and Target Forebay Depths for Ideal Gate-Stroking Solution with Tuned Parameters
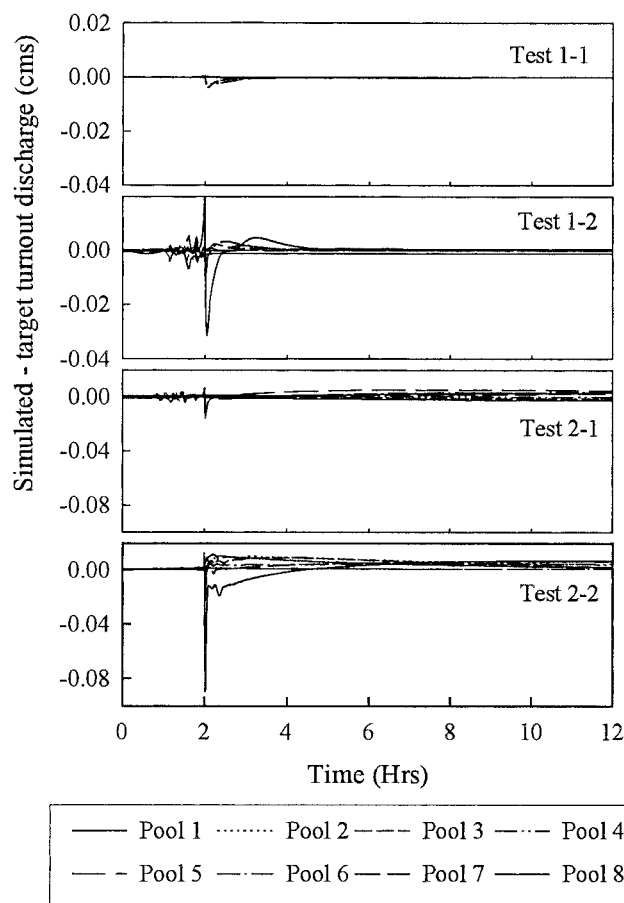
FIG. 3. Difference between Simulated and Target Offtake Flow Rates for Ideal Gate-Stroking Solution with Tuned Parameters

from their targets. From a practical standpoint, the depth and discharge errors are inconsequential: Simulated depths (Fig. 2) deviate from their targets typically by 3 cm or less while the impact on simulated turnout flows (Fig. 3) is even smaller due to the square root relationship between offtake flow and depth, and to magnitude of the head available to the offtake, $y_{us} - y_{ds}$ in (1) or $y_{us} - y_s$ in (2), relative to offtake's vertical opening.

Application of the gate-stroking solutions to Test Canals 1-1 and 2-1 resulted in perturbations to pools downstream from the last turnout with a flow change. These perturbations persist for longer times in the flatter canal, Test 2-1, than for Test 1-1, the steeper canal. This difference is explained by the backwater characteristics of the canals. Because the pools of Test 1-1 are only partially affected by backwater, whereas the canal of Test 2-1 is entirely under backwater effects, the transient flow friction slope is likely to be much smaller for the latter canal than for the former canal. Therefore, disturbances attenuate more slowly under the conditions of Test 2-1.

The task committee defined several performance indicators to compare alternative control algorithms (Clemmens et al. 1998). These performance indicators are the maximum abso-

lute error (MAE), integrated absolute error (IAE), steady-state error (StE), and integrated absolute discharge change (IAQ)

$$MAE = \frac{\max|y_t - y_{target}|}{y_{target}} \quad (8)$$

$$IAE = \frac{\dfrac{\Delta t}{T} \displaystyle\sum_{t=\Delta t}^{T} |y_t - y_{target}|}{y_{target}} \quad (9)$$

$$StE = \frac{\max(|\overline{y_{t=10,12}} - y_{target}|, |\overline{y_{t=22,24}} - y_{target}|)}{y_{target}} \quad (10)$$

$$IAQ = \sum_{t=t_1}^{t_2} (|Q_t - Q_{t-1}|) - |Q_{t_1} - Q_{t_2}| \quad (11)$$

In the previous expressions, y_t and Q_t = the observed depth and check flow at time t, respectively; y_{target} = forebay target depth; T = duration of the test period; Δt = regulation time step; $\bar{y}$ = average depth over the indicated 2-h period (e.g., from 10 to 12 h); Q_{t_1} = discharge at the beginning of the test period; and Q_{t_2} = discharge at the end of the test period. The first three indicators measure deviations with respect to the target depth. The last one is related to the total effort needed to produce the desired transient. Note that (9) differs from the IAE definition provided by Clemmens et al. (1998). In that reference, the summation's lower bound is incorrectly set at $t = 0$. An additional indicator, the integrated delivery error (IDE), was defined for this study as the average, absolute offtake flow q deviations relative to the target offtake flow, q_{target}

$$IDE = \frac{\Delta t}{T} \sum_{t=\Delta t}^{T} \frac{|q_t - q_{target}|}{q_{target}} \quad (12)$$

If $q_{target} = 0$, then IDE is by definition equal to zero.

Performance indicators were calculated for each pool and test case. Table 1 summarizes the average and maximum values from the eight pools in each canal. For three of the tests, the average MAE indicator was 1% or less, whereas the maximum MAE value was 3.6%. Note also that the IAE values were similar to the computed StEs for all tests, with average values of 0.4% or less. Because the depth deviations were small, the simulated offtake deliveries were also close to their targets (small IDE indicators for all tests, with a maximum value of 0.5% for one pool in Test 2-2). Altogether, these results show that the ideal gate-stroking solutions can deliver the desired flow changes while keeping the water levels very close to the target under all test case conditions. It is important to observe, however, that the MAE values of Table 1 may underestimate the actual maximum deviations because only one depth value per regulation interval is used in the calculations. Also, although the steady-state errors should be equal to zero, this is not true for any of the tests. These steady-state errors, which are as large as 0.7% for one pool in Test 1-2, are the results of check and offtake gate position roundoff errors and other numerical inaccuracies.

The IAQ attempts to measure the magnitude of the check flow oscillations produced by a control scheme. It is a measure

TABLE 1. Performance Parameters for Ideal-Stroking Solution

Performance parameter (1)	Test 1-1		Test 1-2		Test 2-1		Test 2-2	
	Average (2)	Maximum (3)	Average (4)	Maximum (5)	Average (6)	Maximum (7)	Average (8)	Maximum (9)
MAE	0.6%	1.7%	1.6%	3.6%	0.3%	0.7%	1.0%	1.7%
IAE	0.1%	0.1%	0.3%	0.6%	0.1%	0.2%	0.4%	0.5%
StE	0.1%	0.1%	0.3%	0.7%	0.2%	0.3%	0.3%	0.6%
IAQ (cm)	0.00	0.01	1.00	1.96	2.71	16.37	1.00	1.96
DE	0.0%	0.1%	0.2%	0.3%	0.1%	0.2%	0.4%	0.5%

that may be more applicable when contrasting feedback control systems. In such cases, the magnitude of the flow overshoot or undershoot cannot be predicted during the controller design process. When applied to the ideal gate-stroking solution, the IAQ can be taken as a measure of the difficulty of producing the desired transient. Note, for example, that larger IAQ values were computed for Test 2-1 than for Test 2-2, even though the latter example requires flow changes in more turnouts and changes of greater magnitude. This is not surprising if one considers, first, that nearly the same length of the canal is affected by the transient in both tests (24 km for Test 2-1 versus 28 km for Test 2-2). Moreover, the transient of 2-1 starts close to normal flow conditions. Strelkoff et al. (1998) have established that canal pools are more difficult to control when the forebay target level is close to normal conditions, and thus, when the amount of backwater storage is small.

Delivery Performance with Approximate Gate-Stroking Schedules—Tuned Regulator

Fig. 4 illustrates the discrete gate-stroking solutions. The corresponding downstream depth and turnout flow errors and the resulting performance indicators appear, respectively, in Figs. 5 and 6 and Table 2. Simulations results show larger depth variations with the approximate schedules than with the ideal schedules (Figs. 5 and 2, respectively) and this is reflected in the computed MAE values (Tables 2 and 1). However, the integrated and steady errors remain under 1% (except for the maximum StE error for Test 1-2, which is 1.1%) and the effect on offtake delivery is also negligible, as demonstrated by computed IDE parameters. Hence, the proposed approximate schedule can adequately handle the scheduled flow changes specified by the task committee test cases. The average StE error for Test 2-1 in Table 2 suggests a slight improvement with respect to the performance from the ideal gate-
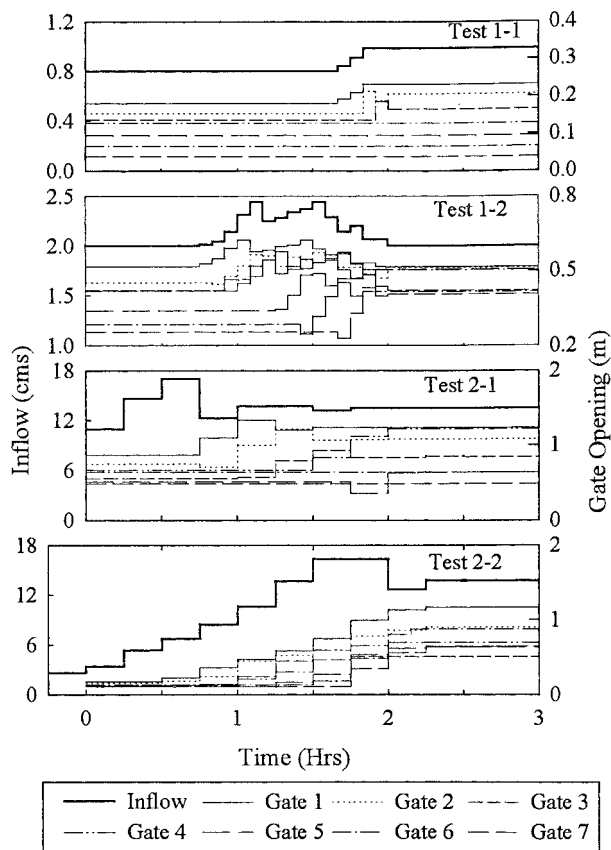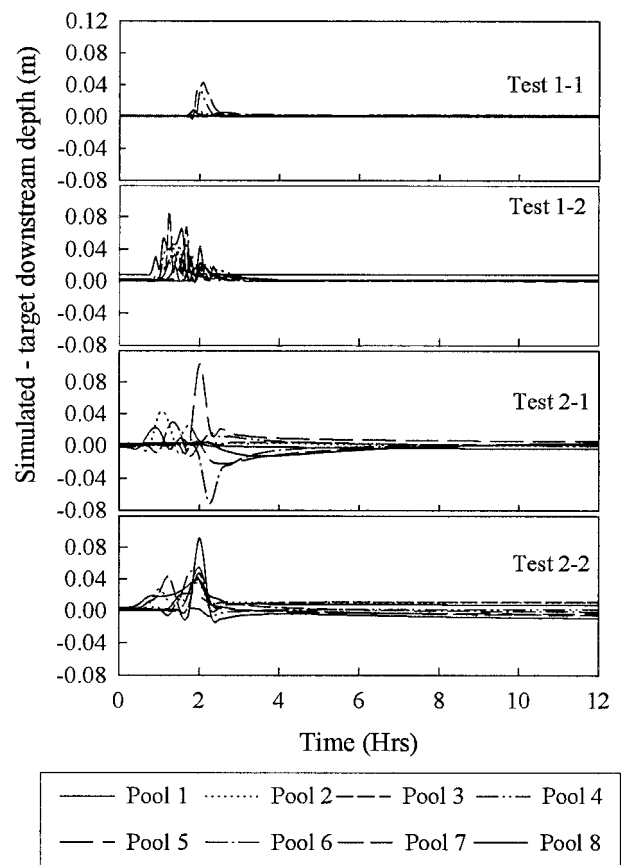

FIG. 5. Difference between Simulated and Target Forebay Depths for Approximate Gate-Stroking Solution with Tuned Parameters

stroking solution, but this result is fortuitous and related to modeling imprecisions.

Delivery Performance with Simple Nonanticipatory Open-Loop Control

The results of the previous section provide an indication of the change in performance of the gate-stroking solution when applied in approximate form. Other approximate gate-stroking schedules can be obtained by applying different constraints on the frequency and magnitude of the gate changes. Rather than examining how the delivery performance would change with other discrete schedules, it seemed more relevant to determine a lower bound for the performance of the feedforward control system. This lower bound can be found by analyzing the performance of a particular nonanticipatory, open-loop control scheme. In this scheme, turnout flow changes are immediately compensated by equivalent flow changes at all upstream check structures. Thus, if more than one turnout flow change is made at a given time, then the discharge increment applied at a check structure is equal to the sum of all turnout increments downstream from that structure. In the following discussion this strategy is referred to as nonanticipatory control.

Figs. 7 and 8 depict the forebay depth and turnout flow errors obtained with nonanticipatory control. Note that the vertical scales on these figures is much greater than on Figs. 2, 3, 5, and 6. As expected, the resulting MAE performance indicators (Table 3) are greater than those obtained with the ideal and approximate gate-stroking solutions (Table 2). An exception is the maximum MAE for Test 2-1, which is smaller with no anticipation but, as noted earlier, this indicator may not be adequately estimated when using a large sampling interval. For the two tests on Canal 1, the StE indicators (Table 3) are similar in magnitude relative to the values presented in Tables 1

FIG. 4. Approximate Inflow and Gate Opening Schedules

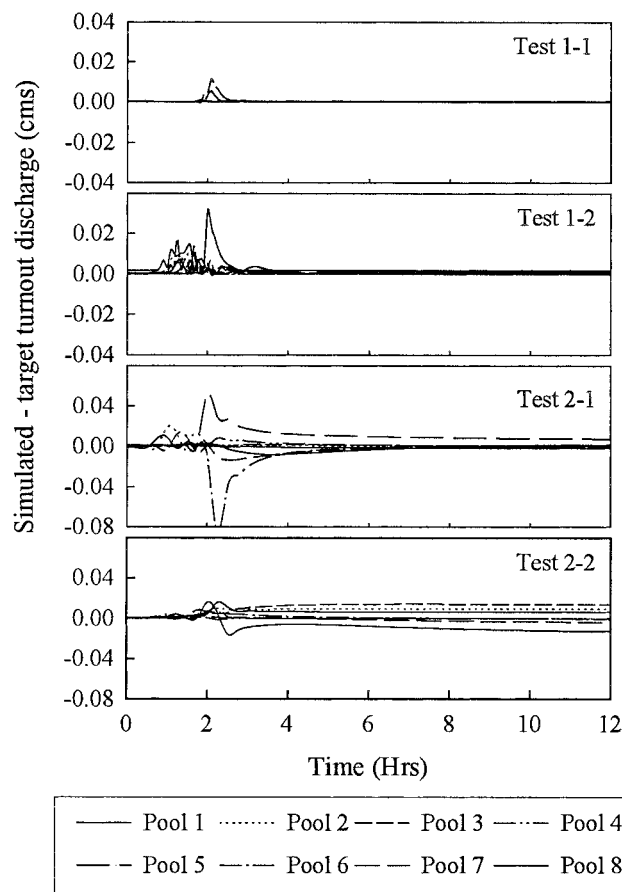| Performance parameter (1)	Test 1-1		Test 1-2		Test 2-1		Test 2-2	
	Average (2)	Maximum (3)	Average (4)	Maximum (5)	Average (6)	Maximum (7)	Average (8)	Maximum (9)
MAE	1.5%	5.4%	5.3%	10.8%	2.1%	5.4%	2.4%	5.4%
IAE	0.2%	0.3%	0.5%	1.1%	0.2%	0.5%	0.4%	0.5%
StE	0.1%	0.2%	0.3%	0.9%	0.1%	0.3%	0.3%	0.5%
IAQ (cm)	0.05	0.20	0.79	1.25	2.55	10.66	0.99	7.46
DE	0.1%	0.2%	0.4%	0.7%	0.3%	0.4%	0.3%	0.5%

FIG. 6. Difference between Simulated and Target Offtake Flow Rates for Approximate Gate-Stroking Solution with Tuned Parameters

FIG. 7. Difference between Simulated and Target Forebay Depths for Nonanticipatory Open-Loop Control Scheme with Tuned Parameters

and 2, meaning that near-steady flow conditions are restored quickly. As a result, the integrated depth and delivery errors are also similar to those obtained with the ideal and approximate gate-stroking schedules. On the other hand, the StE indicators for the tests on Canal 2 are greater, by an order of magnitude, than the corresponding values in Tables 1 and 2. Thus, the IAE and IDE indicators are also significantly greater.

This difference in performance of the nonanticipatory control scheme between the two canals is explained mainly by the magnitude of the pool volume changed needed in each case to produce the new steady flow condition and, to a lesser degree, to differences in the canal's dynamic properties. Table 4 summarizes the pool volume change resulting from each test case as well as the time needed to provide this volume change based on the final inflow rate. Thus, for both tests on Canal 1, it takes 10 min to supply the compensating volume (assuming constant offtake deliveries), whereas significantly more time is needed to supply this volume for Tests 2-1 and 2-2. The new steady-state hydraulic grade line cannot be attained until these changes in volume have been completed. A nonanticipatory control method that accounts for these pool vol-
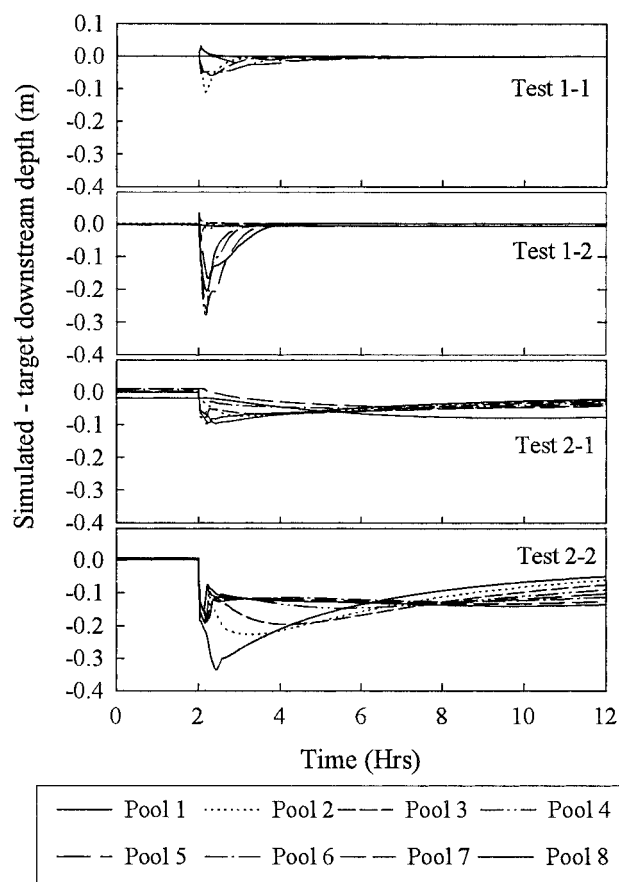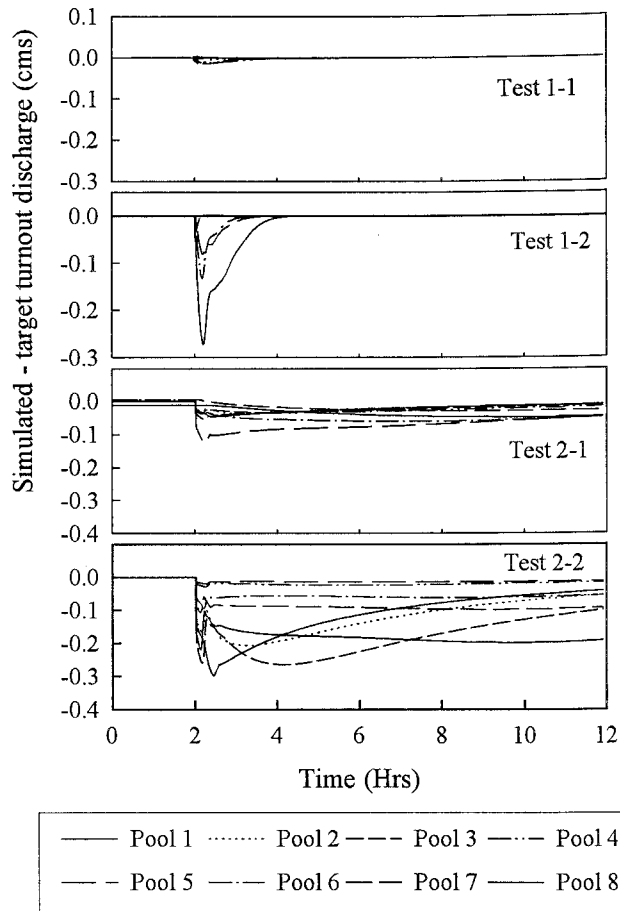
ume changes would be expected to provide better control than the method discussed herein (Parrish 1997).

The Froude number F (the ratio of the inertial to gravitational forces) is also a factor that affects the open-loop controllability of a canal (Strelkoff et al. 1998; Bautista et al. 1996). Using a nondimensional gate-stroking model, Bautista et al. compared the shape of gate-stroking solutions for a wide range of single-pool canal configurations and flow conditions. Their results show the influence of F on the shape of the gate-stroking solutions. As F increases (in the subcritical range 0.4–0.9), the shape of the solution inflow hydrograph tends to duplicate the shape of the demand outflow hydrograph. With decreasing values of F, larger inflow variations are required to produce a desired downstream flow variation, and thus, it becomes more difficult to maintain the target forebay water levels with nonanticipatory control. For the test cases, F ranges from 0.68 to 0.80 for Canal 1, under the initial flow conditions, and from 0.16 to 0.14 for Canal 2, primarily as a result of differences in slope. This difference in F and the delay in volume compensation helps to explain the relative results between Canals 1 and 2. In terms of steady state and integrated

TABLE 3. Performance Parameters for Simple Nonanticipatory Control Scheme

Performance parameter (1)	Test 1-1		Test 1-2		Test 2-1		Test 2-2	
	Average (2)	Maximum (3)	Average (4)	Maximum (5)	Average (6)	Maximum (7)	Average (8)	Maximum (9)
MAE	4.4%	12.2%	14.4%	34.4%	4.0%	5.3%	10.0%	15.4%
IAE	0.4%	0.6%	0.9%	1.7%	2.2%	3.1%	5.6%	6.2%
StE	0.1%	0.1%	0.4%	0.7%	2.2%	4.6%	5.5%	8.1%
IAQ(cm)	0.02	0.05	0.07	0.16	0.14	0.42	0.33	0.75
DE	0.4%	0.7%	0.8%	1.9%	2.3%	3.3%	6.6%	7.7%

FIG. 8. Difference between Simulated and Target Offtake Flow Rates for Nonanticipatory Open-Loop Control Scheme with Tuned Parameters

TABLE 4. Volume Change, Final Inflow Rate, and Volume Compensation Time for Each Test

Variable (1)	Test 1-1 (2)	Test 1-2 (3)	Test 2-1 (4)	Test 2-2 (5)
Volume change (m³)	168	1,024	18,955	52,244
Final inflow rate (m³/s)	1.0	2.0	13.5	13.7
Minimum time to supply compensating volume (min)	3	9	23	64

and the requested flow change. In this way, operators do not have to concern themselves with differences between the discharge measured at the check structure and the sum of all outflows measured downstream from it. Simulations with the untuned parameters were conducted by applying incremental flow changes starting from an assumed (based on the incorrect head discharge relationship) steady-state discharge at each check gate, just as the operator in a remote supervisory controlled system would do. Alternate incremental approaches were also tried, but results were indistinguishable from those presented for this case.

A steady-state simulation was performed with CanalCAD to obtain the initial steady-state profile with the actual (unknown to the operator) gate discharge coefficients and Manning's n values. Initial gate positions were computed from these results. These gate positions, along with the assumed (incorrect) hydraulic parameters and the CanalCAD-computed afterbay depths, were then used to compute the initial flows assumed by the operators. The schedules of flow changes obtained from the originally computed ideal gate-stroking solutions were then added to these assumed initial flows. The new approximate schedules were generated using the same constraints as before on the regulation interval and minimum gate movement.

Figs. 9 and 10 show, respectively, the forebay level and turnout flow errors computed with the untuned parameters, while the performance indicators for these tests are summarized in Table 5. As expected, the performance of the gate-stroking solutions is not as favorable under the untuned conditions when compared with the tuned controller results. In particular, the steady-state errors shown in Table 5 are an order or magnitude greater than those presented in Table 2. The inaccurate gate hydraulic relationships are the key factor influencing these steady-state errors. The loss of performance is greatest for the two test cases on Canal 2, not only because they involve larger flow changes than the Canal 1 tests, but also because the check gates for the former canal are submerged. The relationship between gate opening and discharge for submerged gates is very nonlinear because the discharge varies with the water level upstream and downstream from the gate, and the downstream depth varies with the changing discharge. For the two tests on Canal 2, the StE values dictate the magnitude of the MAE performance indicator and these steady errors continue to grow after 12-h test period.

The effect of the untuned Manning's n is most evident from the results of Test 1-2. In this case, the flow increase to the last pool arrives later than expected, resulting in a temporarily large delivery error (Fig. 10). This delay in wave arrival also

errors, greater benefits can be expected from using gate-stroking or any other volume-compensating anticipatory control method on the low-Froude number, Canal 2, than on the high-Froude number, Canal 1. However, higher short-duration water level errors can be expected on the high Froude number canal.

Delivery Performance with Approximate Gate-Stroking Schedules—Untuned Results

In real water delivery systems, flow measurement is uncertain to a lesser or greater degree. Operators compensate for this uncertainty by making flow and gate changes incrementally. For a given flow change request at an offtake, they try to make an equivalent flow adjustment at all check structures upstream from that offtake. In manually controlled systems, they do this by turning the gate wheel a number of times under the assumption that one turn of the wheel provides a more-or-less fixed flow increment; i.e., by assuming that dQ/da is constant over a given range of flow. For delivery systems with remote supervisory control, operators adjust the gate position until the reported flow matches the sum of the initial discharge

explains the computed MAE indicator for this test which, unlike the other test cases, is still significantly greater than the StE indicator. This means that the "transient" period water level deviations for this test are still large in relation to the errors observed during the period of relatively steady flow.

Delivery Performance for All Control Schemes

Fig. 11 summarizes the maximum MAE values computed for all test cases and control schemes. A similar summary is provided in Fig. 12 for the maximum StE performance indicators. These graphs emphasize the similarities between the ideal and approximate gate-stroking solutions, the difference in performance between anticipatory and nonanticipatory open-loop control, and the detrimental effects of inaccurate hydraulic information on the controller's performance. Because the trends in maximum integrated errors IAE and IDE between the various approaches for each test case are very similar to the steady-state errors, they are not shown here.

The ideal and approximate gate-stroking solutions yielded the smallest maximum water level deviations for all tests (Fig. 11). On the other hand, the largest level variations were observed on Canal 1 with the nonanticipatory tests, whereas the untuned tests provided the largest level deviations on Canal 2. The nonanticipatory control tests conducted resulted in steady errors similar to those obtained with anticipatory control on Canal 1, whereas on Canal 2 water levels did not return to their targets within the 12-h test period. For all tests, the primary impact of improperly tuned parameters was relatively large steady-state water-level deviations. For Test 2-2, these steady-state errors were greater than the errors observed during the early part of the transient, when the actual gate changes are being made.

Although the steady-state water level-deviations can be expected to become negligible with increasing time for all tuned parameters tests, the StE indicators of Tests 2-1 and 2-2 with nonanticipatory control were several times greater than with gate-stroking, either ideal or approximate (Fig. 12). For the nonanticipatory control tests, the water surface profile was still changing, very slowly, at the end of the 12-h test period. The water levels for Tests 1-1 and 1-2, on the other hand, essentially stabilized after the fourth hour. Thus, even though storage and levels dropped rapidly in the first canal with nonan-
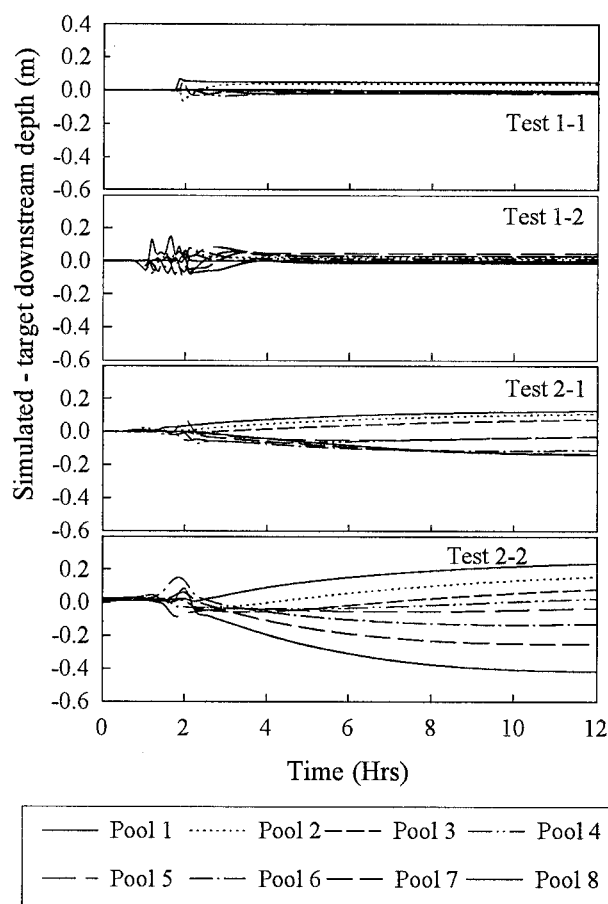

FIG. 9. Difference between Simulated and Target Forebay Depths for Approximate Gate-Stroking Solution with Untuned Parameters
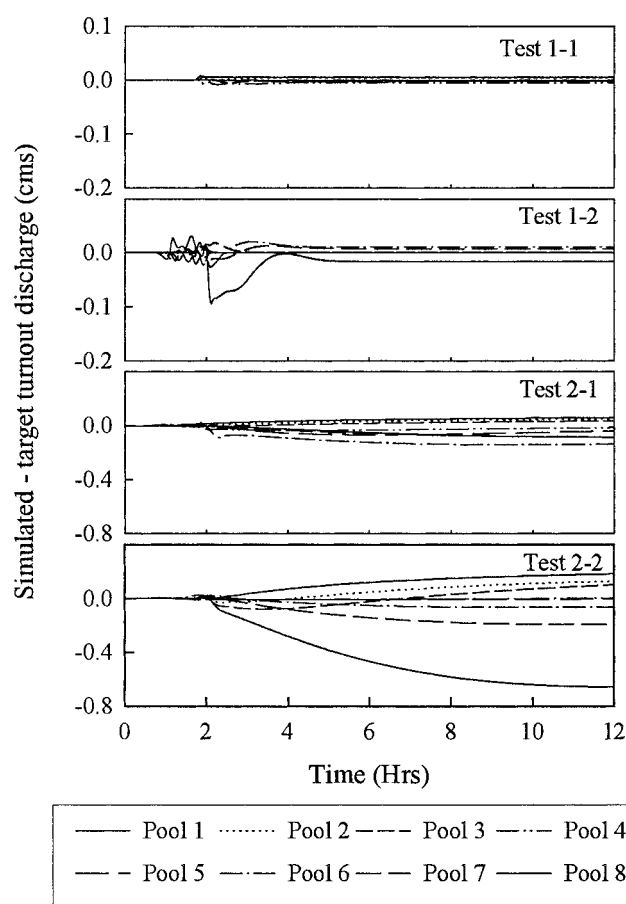

FIG. 10. Difference between Simulated and Target Offtake Flow Rates for Approximate Gate-Stroking Solution with Untuned Parameters

TABLE 5. Performance Parameters for Approximate Untuned Gate-Stroking Solution

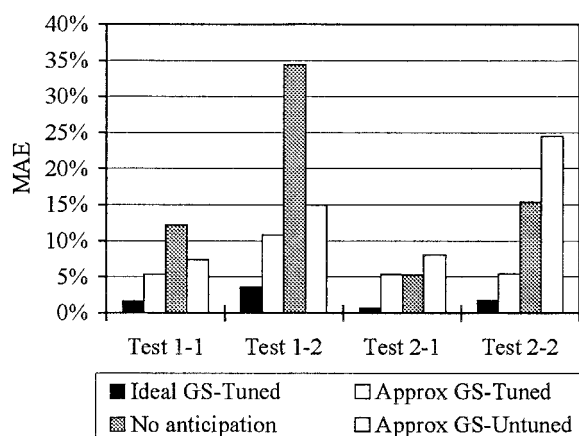| Performance parameter (1)	Test 1-1		Test 1-2		Test 2-1		Test 2-2	
	Average (2)	Maximum (3)	Average (4)	Maximum (5)	Average (6)	Maximum (7)	Average (8)	Maximum (9)
MAE	3.7%	7.4%	9.9%	14.9%	5.6%	8.1%	9.5%	24.5%
IAE	1.7%	4.9%	2.4%	4.6%	3.3%	4.7%	5.6%	15.1%
StE	2.1%	5.7%	2.2%	4.8%	5.0%	8.0%	8.8%	24.3%
IDE	1.7%	4.7%	1.4%	3.4%	3.3%	4.9%	5.9%	17.1%

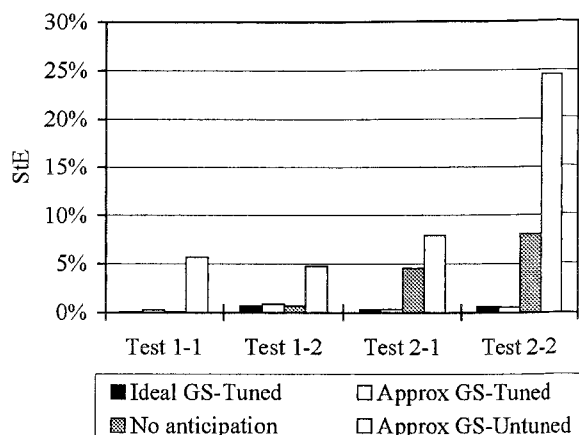**FIG. 11. Maximum MAE Values for All Tests and Control Schemes**

FIG. 12. Maximum IAE Values for All Tests and Control Schemes

ticipatory control, recovery was rapid. Notice in particular the MAE computed for Test 1-2, which was the largest of all computed values, whereas its corresponding StE was comparable with that computed from either of the gate-stroking solutions. For this test, the specified changes in turnout demand require no net change in discharge at the head of the canal. However, reaching the new flow conditions requires a change in canal storage. This change in storage can be quickly compensated by the incoming flow, and thus, the effect of the water deficit is short-lived. Changes in storage for a given depth change are much greater for the second canal than for the first, especially under the conditions of Test 2-1. For this test, the temporary pool volume deficits or excesses caused by the lack of anticipation resulted in depth deviations during the initial part of the transient that were only slightly larger than those observed with the approximate gate-stroking solution (Figs. 5 and 7). Pool levels did not recover during the test period, however, because of the limited supply in relation to the storage change. Thus, the maximum StE was several times larger than the maximum value obtained with gate stroking.

These results, together with the findings of O'Laughlin (1972), Bodley and Wylie (1978), and Bautista et al. (1997), suggest that adequate control can be achieved on canals of significantly different physical characteristics with the gate-stroking solutions, either ideal or approximate. On the other hand, canal physical characteristics play a more significant role in determining the performance of the nonanticipatory control scheme. Well-tuned gate relationships are critical where open-loop flow control is used in the absence of closed-loop feedback control of water levels.

CONCLUSIONS

For the four tests considered in this study, the ideal gate-stroking solutions can maintain a relatively constant forebay target depth (IAE ≤ 0.6%), and thus, deliver the prescribed flow variations with a relatively small error (IDE ≤ 0.5%). The performance of the approximate gate-stroking schedules, which were developed by limiting the frequency and magnitude of gate adjustments, resulted in errors that, although slightly larger than under the idealized anticipatory control case, were still <1% for both the integrated, steady, and delivery errors. For the conditions represented by Canal 1, the nonanticipatory control scheme resulted in larger maximum deviations than with anticipation, although overall performance was not impacted as much due to the rapid response of the canal. For the flow conditions represented by Canal 2 (a system with a slow response), delivery performance can be substantially improved with the help of anticipatory control measures.

Results also show that the sophistication of the gate-stroking method may not be justified in situations where canal model parameters cannot be adequately established, and thus, flows under steady conditions cannot be adequately predicted. Given that canal physical properties will change over time, particularly in the absence of adequate canal maintenance, model parameters need to be recalibrated with some frequency if reasonable performance is expected from any open-loop control algorithm. Because one of the objectives of feedback control procedures is to provide safeguards against open-loop modeling uncertainties, it is clear then that adequate automatic control systems for irrigation canals require the incorporation of both feedback and feedforward control capabilities.

APPENDIX I. REFERENCES

Bautista, E., Clemmens, A. J., and Strelkoff, T. S. (1996). "Characterization of canal operations under ideal anticipatory control." *Proc., of North Am. Water and Envir. Congr.*, ASCE, Reston, Va. (In CD-ROM).

Bautista, E., Clemmens, A. J., and Strelkoff, T. S. (1997). "Inverse computational methods for open-channel flow control." *J. Irrig. and Drain. Engrg.*, ASCE, 123(2), 129–136.

Bodley, W. E., and Wylie, E. B. (1978). "Control of transients in series channel with gates." *J. Hydr. Div.*, ASCE, 10, 1395–1407.

Chevereau, G. (1991). "Contribution a l'etude de la regulation dans les systemes hydrauliques a surface libre," PhD thesis, Institut National Polytechnique de Grenoble, Grenoble, France.

Clemmens, A. J., Kacerek, T. F., Grawitz, B., and Schuurmans, W. (1998). "Recommended test cases for canal control algorithms." *J. Irrig. and Drain. Engrg.*, ASCE, 124(1), 23–30.

Falvey, H. T., and Luning, P. C. (1979). "Gate stroking." *Rep. REC-ERC-79-7*, USDI-U.S. Bureau of Reclamation, Washington, D.C.

Holly, F. M., Jr., and Parrish, J. B. (1995). "CanalCAD: Dynamic flow simulation in irrigation canals with automatic gate control." Iowa Institute of Hydraulic Research, Iowa City, Iowa.

Liu, F., Feyen, J., and Berlamont, J. (1992). "Computational method for regulating unsteady flow in open channels." *J. Irrig. and Drain. Engrg.*, ASCE, 118(10), 674–689.

O'Laughlin, E. (1972). "Application of unsteady flow analysis to operation decisions in long aqueducts." Proc., ICID 8th Congr., R16, Sofia Bulgaria. 28.2.207–28.2.223.

Parrish, J. B. (1997). "Idealized automated control of sloping canals." *J. Irrig. and Drain. Engrg.*, ASCE, 123(4), 270–278.

Strelkoff, T. S., Deltrour, J. L., Burt, C. M., Clemmens, A. J., and Baume, J. P. (1998). "Influence of canal geometry and dynamics on controllability." *J. Irrig. and Drain. Engrg.*, ASCE, 124(1), 16–22.

Wylie, E. B. (1969). "Control of transient free surface flow." *J. Hydr. Div.*, ASCE, 95(1), 347–361.

APPENDIX II. NOTATION

The following symbols are used in this paper:

a = check gate vertical opening;
B = check gate width;
H = upstream depth above gate sill;

K = variable in turnout head-discharge relationship;
Q_G = gate discharge;
Q_l = gate leakage;
Q_t = check flow at time t;
Q_{t_1} = check discharge at beginning of test period;
Q_{t_2} = check discharge at end of test period;
q = turnout discharge;
T = duration of control test period;
$\bar{y}$ = average depth;
y_{ds} = depth downstream of check gate;

y_s = gate sill elevation relative to canal invert;
y_t = depth at time t;
y_{target} = forebay target depth;
y_{us} = depth upstream from check gate;
y_0 = head downstream of turnout;
Δt = control time step;
ε = check gate dimensionless variable vertical contraction coefficient; and
μ = check gate dimensionless constant horizontal contraction coefficient.